Influence of Alkali Metal Cation (Li(I), Na(I), K(I)) on the Construction of Chiral and Achiral Heterometallic Coordination Polymers

6 AUTHORS, INCLUDING:

Li Ma
City University of Hong Kong
23 PUBLICATIONS **301** CITATIONS

SEE PROFILE

Li Liang
Dalian University of Technology
83 PUBLICATIONS **2,239** CITATIONS

SEE PROFILE

George E Kostakis
University of Sussex
87 PUBLICATIONS **1,433** CITATIONS

SEE PROFILE

Influence of Alkali Metal Cation (Li(I), Na(I), K(I)) on the Construction of Chiral and Achiral Heterometallic Coordination Polymers

Guo Peng,[†] Li Ma,[†] Jinbiao Cai,[†] Li Liang,[†] Hong Deng,*[,†] and George E. Kostakis*[,‡]

[†]School of Chemistry & Environment and Key Laboratory of Electrochemical Technology on Energy Storage and Power Generation in Guangdong Universities, South China Normal University, Guangzhou 510006, P. R. China

[‡]Institute of Nanotechnology, Karlsruhe Institute of Technology, Postfach 3640, D-76021 Karlsruhe, Germany

S *Supporting Information*

ABSTRACT:
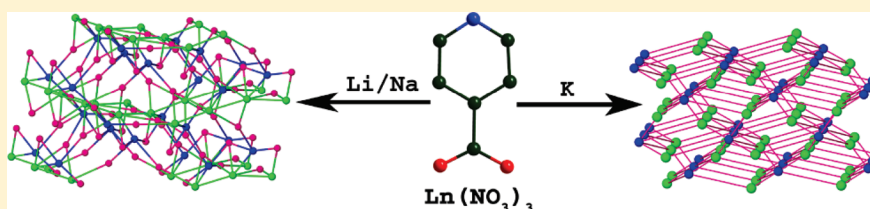
A series of chiral and achiral lanthanide-alkali coordination polymers, $[LnM(INA)_3(OAc)]$ where $[M = Li, Ln = Eu$ (**1**); $M = Li, Ln = Tb$ (**2**); $M = Na, Ln = Eu$ (**3**); $M = Na, Ln = Tb$ (**4**); INA = isonicotinate; OAc = acetate] and $[TbK(INA)_2(OAc)_2]$ (**5**), have been solvothermally synthesized and structurally characterized. The acetate groups were in situ obtained from oxidation of CH_3CN during the reaction. Structures with remarkably different connectivities are formed when Li(I), Na(I), and K(I) were introduced into the system. Compounds **1**−**4** are isostructural three-dimensional (3D) coordination polymers and built up by right-/left-handed Ln-O-M chiral helicals and INA linkers possessing a **3,3,4,7T2** topology. Compound **5** is a 3D pillared coordination polymer constructed from two-dimensional (2D) Tb−O−K layers with INA as connectivities possessing an **alb-4,8-P21/c** topology. Circular dichroism (CD) measurements confirmed that the resulting crystals of **1**, **3**, and **4** were racemic mixtures. The photoluminescent properties of compounds **1**−**5** were investigated, exhibiting intense characteristic emission spectra of lanthanide ions.

■ INTRODUCTION

The design, synthesis, and investigation of chiral coordination polymers are currently an interesting area of research stimulated by their potential applications in enantioselective separations and catalysis,[1] nonlinear optical and ferroelectric materials,[2] magneto-chiral materials,[3] and biomimetic chemistry.[4] Generally, chiral coordination polymers can be built from chiral ligands or by spontaneous resolution without any chiral auxiliary. On the basis of the first method, numerous chiral coordination polymers have been obtained.[5] However, chiral coordination polymers generated by spontaneous resolution without any chiral sources are still rare.[6] The preparation of chiral coordination polymers from achiral ligands is an important topic to study the generation of chirality in biological systems. Though extensive studies have been performed and various hypotheses have been brought up,[7] the origin of homochirality remains a subject of much debate in biology. The alkali metal cations play a key role in nature; for instance, alkali cations Li(I), Na(I), and K(I) have very specific functions such as the regulation of the ionic equilibrium of living cells in our body. Thus, the study of chiral coordination polymers induced by alkali metal cation increases knowledge of chiral generation in biology. Up to now, several chiral coordination polymers which contain both lanthanide and alkali metal have been reported.[8] For instance, Majeed et al.

reported two lanthanide-alkali coordination polymers possessing novel **srs** chiral topology derived solely from benzoate,[8a] while Sendor et al. obtained a series of chiral Ln-Na coordination polymers with interesting luminescent properties.[8c] However, an extended literature survey shows that a systematic study of the influence of the alkali metal ions on the construction of lanthanide-alkali coordination polymers has not been reported before.

Inspired by the aforementioned considerations and our previous work on heterometallic coordination polymers,[9] in the present paper, the syntheses, structure determination, and topological evaluation of a series of three-dimensional (3D) heterometallic Ln-M (M = Li(I), Na(I) and K(I)) compounds, namely, $[LnM(INA)_3(OAc)]$ where $[M = Li, Ln = Eu$ (**1**); $M = Li, Ln = Tb$ (**2**); $M = Na, Ln = Eu$ (**3**); $M = Na, Ln = Tb$ (**4**); INA = isonicotinate; OAc = acetate] and $[TbK(INA)_2(OAc)_2]$ (**5**), are described. The thermal stability, photoluminescent, and circular dichroism (CD) properties of these coordination polymers have also been investigated.

Table 1. Crystallographic Data for Compounds 1–5

	1	2	3	4	5
empirical formula	$C_{20}H_{15}EuLiN_3O_8$	$C_{20}H_{15}TbLiN_3O_8$	$C_{20}H_{15}EuNaN_3O_8$	$C_{20}H_{15}TbNaN_3O_8$	$C_{16}H_{14}TbKN_2O_8$
formula weight	584.25	591.21	600.30	607.26	560.31
crystal system	$P6_122$	$P6_522$	$P6_522$	$P6_122$	$P2_1/n$
space group	hexagonal	hexagonal	hexagonal	hexagonal	monoclinic
a (Å)	11.3891(6)	11.3686(3)	11.6684(3)	11.6202(7)	10.6936(9)
b (Å)	11.3891(6)	11.3686(3)	11.6684(3)	11.6202(7)	14.7020(12)
c (Å)	26.872(3)	26.7353(12)	27.7140(16)	27.550(3)	12.9661(11)
α (°)	90	90	90	90	90
β (°)	90	90	90	90	106.3130(10)
γ (°)	120	120	120	120	90
V (Å^3)	3018.6(4)	2992.47(17)	3267.8(2)	3221.7(5)	1956.4(3)
Z	6	6	6	6	4
D_{calcd} (g cm^{-3})	1.928	1.968	1.830	1.878	1.902
μ (mm^{-1})	3.172	3.601	2.951	3.366	3.873
$F(000)$	1716	1728	1764	1776	1088
reflns collected	18732	18574	20187	20053	9869
unique reflns	2391	2362	2146	2557	3523
GOF	1.082	1.133	1.053	1.063	1.043
R_{int}	0.0280	0.0338	0.0858	0.0477	0.0319
R_1 $[I > 2\sigma(I)]^a$	0.0157	0.0165	0.0415	0.0202	0.0240
wR_2 (all data)^b	0.0370	0.0389	0.0858	0.0433	0.0572
Flack parameter	−0.005(13)	−0.014(13)	−0.02(3)	−0.010(13)	

$^a R_1 = \Sigma|F_0| - |F_c||/\Sigma|F_0|.$ $^b wR_2 = \{\Sigma[w(F_0^2 - F_c^2)^2]/\Sigma w(F_0^2)^2\}^{1/2}.$

■ EXPERIMENTAL SECTION

Materials and Instruments. All the materials and reagents are commercially available and were used without further purification. Elemental (C, H, N) analyses were performed on a Perkin–Elmer 2400 element analyzer. Infrared (IR) samples were prepared as KBr pellets, and spectra were obtained in the 4000–400 cm^{-1} range using a Nicolet Avatar 360 FT-IR spectrophotometer. Thermogravimetric analysis (TGA) experiments were carried out on a Perkin–Elmer TGA 7 thermogravimetric analyzer with the heating rate of 10 °C/min from 35 to 750 °C under dry air atmosphere. Powder X-ray diffraction (PXRD) investigations were carried out on a Philips PW-1830 X-ray diffractometer with CuKα radiation. Solid-state circular dichroism (CD) spectra were recorded on a JASCO J-810 spectropolarimeter with KCl pellets. Fluorescence spectra were recorded with an Edinburgh FLS920 spectrophotometer analyzer.

Synthesis of [EuLi(INA)₃(OAc)] (1). A mixture of LiCl (0.021 g, 0.5 mmol), Eu(NO₃)₃·6H₂O (0.223 g, 0.5 mmol), HINA (0.185 g, 1.5 mmol), and CH₃CN (10 mL) was sealed in a 23 mL Teflon-lined stainless-steel autoclave and heated to 170 °C for 3 days and then cooled to room temperature at 5 °C/h. Colorless rod-shaped crystals were isolated by filtration (yield 28% based on Eu), washed with CH₃CN, and dried in air. Pure phase crystals of **1** were obtained by manual separation. Elemental Anal. Calcd (%) for **1**, C₂₀H₁₅EuLi N₃O₈: C, 41.11; H, 2.59; N, 7.19; found: C, 41.40; H, 2.62; N, 7.03. IR data (KBr cm^{-1}): 3394(w), 1651(m), 1604(m), 1539(s), 1408(m), 1317(w), 1222(w), 1061(w), 1008(w), 951(w), 859(w), 798(m), 769(m), 674(w), 649(w).

Synthesis of [TbLi(INA)₃(OAc)] (2). Compound **2** was synthesized by a procedure similar to that of **1**, except that Eu(NO₃)₃·6H₂O was replaced by Tb(NO₃)₃·6H₂O (0.227 g 0.5 mmol). Colorless rod-shaped crystals were isolated by filtration (yield 25% based on Tb), washed with CH₃CN, and dried in air. Pure phase crystals of **2** were obtained by manual separation. Elemental Anal. Calcd (%) for **2**, C₂₀H₁₅TbLi N₃O₈: C, 40.63; H, 2.56; N, 7.11; found: C, 40.27; H, 2.42; N, 7.43. IR data (KBr cm^{-1}): 3397(w), 1656(w), 1596(m),

1542(s), 1393(s), 1323(w), 1222(w), 1055(w), 1008(w), 956(w), 865(w), 798(w), 766(m), 678(w), 615(w).

Synthesis of [EuNa(INA)₃(OAc)] (3). Compound **3** was synthesized by a procedure similar to that of **1** except that LiCl was replaced by Na₂C₂O₄ (0.067 g, 0.5 mmol). Yellow octahedron-shaped crystals were isolated by filtration (yield 46% based on Eu), washed with CH₃CN, and dried in air. Pure phase crystals of **3** were obtained by manual separation. Elemental Anal. Calcd (%) for **3**, C₂₀H₁₅EuN₃NaO₈: C, 40.02; H, 2.52; N, 7.00; found: C, 40.29; H, 2.35; N, 7.26. IR data (KBr cm^{-1}): 3414(w), 1627(m), 1594(m), 1547(s), 1399(s), 1317(w), 1222(w), 1055(w), 1006(w), 811(w), 764(m), 681(w).

Synthesis of [TbNa(INA)₃(OAc)] (4). Compound **4** was synthesized by a procedure similar to that of **1** except that LiCl and Eu-(NO₃)₃·6H₂O were replaced by Na₂C₂O₄ (0.067 g, 0.5 mmol) and Tb(NO₃)₃·6H₂O (0.227 g, 0.5 mmol). Yellow octahedron-shaped crystals were isolated by filtration (yield 41% based on Tb), washed with CH₃CN, and dried in air. Pure phase crystals of **4** were obtained by manual separation. Elemental Anal. Calcd (%) for **4**, C₂₀H₁₅TbN₃NaO₈: C, 39.56; H, 2.49; N, 6.92; found: C, 40.01; H, 2.28; N, 7.13. IR data (KBr cm^{-1}): 3410(w), 1630(m), 1589(m), 1548(s), 1396(s), 1317(w), 1228(w), 1055(w), 1008(w), 804(w), 767(m), 678(w).

Synthesis of [TbK(INA)₂(OAc)₂] (5). A mixture of KI (0.083 g, 0.5 mmol), Tb(NO₃)₃·6H₂O (0.227 g, 0.5 mmol), HINA (0.185 g, 1.5 mmol), and CH₃CN (10 mL) was sealed in a 23 mL Teflon-lined stainless-steel autoclave and heated to 170 °C for 3 days and then cooled to room temperature at 5 °C/h. Colorless prismatic crystals were isolated by filtration (yield 32% based on Tb), washed with CH₃CN, and dried in air. Pure phase crystals of **5** were obtained by manual separation. Elemental Anal. Calcd (%) for **5**, C₁₆H₁₄KN₂O₈Tb: C, 34.30; H, 2.52; N, 5.00; found: C, 33.97; H, 2.81; N, 4.83. IR data (KBr cm^{-1}): 2958(w), 1680(w), 1588(m), 1539(m), 1417(s), 1259(m), 1223(w), 1092(w), 1019(w), 867(w), 795(m), 694(w), 674(w).

Single-Crystal Structure Determination. Single crystal XRD data collections of **1**–**5** were performed on a Bruker Apex II CCD

Table 2. Selected Bond Lengths (Å) for Compounds 1−5[a]

1			
Eu(1)−O(2)#1	2.3400(17)	Eu(1)−O(3)	2.352(2)
Eu(1)−O(1)	2.4530(17)	Eu(1)−O(4)	2.4832(18)
Li(1)−O(4)	2.084(3)	Li(1)−N(1)#2	2.169(5)
2			
Tb(1)−O(1)#4	2.459(2)	Tb(1)−O(2)#4	2.4329(18)
Tb(1)−O(3)#3	2.3140(19)	Tb(1)−O(4)#4	2.328(2)
Li(1)−O(1)	2.066(3)	Li(1)−N(1)#5	2.181(6)
3			
Eu(1)−O(2)#6	2.350(5)	Eu(1)−O(3)	2.360(5)
Eu(1)−O(1)	2.440(4)	Eu(1)−O(4)	2.493(5)
Na(1)−O(4)	2.201(5)	Na(1)−N(1)#7	2.456(7)
Na(1)−O(2)	2.742(6)		
4			
Tb(1)−O(1)#1	2.323(2)	Tb(1)−O(3)#8	2.333(2)
Tb(1)−O(2)#8	2.410(2)	Tb(1)−O(4)#8	2.468(2)
Na(1)−O(4)	2.190(2)	Na(1)−N(1)#2	2.451(3)
Na(1)−O(1)	2.738(3)		
5			
Tb(1)−O(1)	2.496(3)	Tb(1)−O(2)	2.431(2)
Tb(1)−O(3)	2.435(3)	Tb(1)−O(4)	2.502(2)
Tb(1)−O(5)	2.375(2)	Tb(1)−O(6) #10	2.361(2)
Tb(1)−O(7)	2.568(2)	Tb(1)−O(7) #10	2.299(2)
Tb(1)−O(8)	2.442(3)	K(1)−O(1)	2.664(3)
K(1)−O(2)#9	2.698(3)	K(1)−O(4)#9	2.780(3)
K(1)−O(6)#10	2.967(3)	K(1)−N(1)#11	3.008(4)
K(1)−N(2)#12	3.058(4)	K(1)−O(5)#9	3.162(3)

[a] Symmetry codes: #1 $x, x − y + 2, −z + 1/6$; #2 $y, −x + y + 1, z − 1/6$; #3 $−y, −x, −z + 1/6$; #4 $x − y, −y, −z$; #5 $x − y, x − 1, z − 1/6$; #6 $y, −x + y + 1, z + 1/6$; #7 $x − y + 1, −y + 1, −z + 1$; #8 $x − y + 1, −y + 2, −z$; #9 $x − 1/2, −y + 1/2, z − 1/2$; #10 $−x + 1, −y, −z$; #11 $−x + 1, −y + 1, −z$; #12 $x − 1, y, z$.

diffractometer operating at 50 kV and 30 mA using MoKα radiation (λ = 0.71073 Å). Data collection and reduction were performed using the APEX II software.[10] Multiscan absorption corrections were applied for all the data sets using the APEX II program.[10] All structures were solved by direct methods and refined by full-matrix least-squares on F^2 using the SHELXTL program package.[10] All non-hydrogen atoms were refined with anisotropic displacement parameters. Hydrogen atoms attached to carbon were placed in geometrically idealized positions and refined using a riding model. Hydrogen atoms on water molecules were located from difference Fourier maps and were also refined using a riding model. Crystallographic data for 1−5 are listed in Table 1, and selected bond lengths for all compounds are given in Table 2. CCDC numbers: 794308−794312 for compounds 1−5.

■ RESULTS AND DISCUSSION

Syntheses. The series compounds were obtained by the solvothermal reaction of HINA, $Ln(NO_3)_3 \cdot 6H_2O$, and alkali metal salts in the mixture of CH_3CN. An interesting feature in the molecular formulas of those compounds is the existence of acetate anions which can be in situ formed from the partial
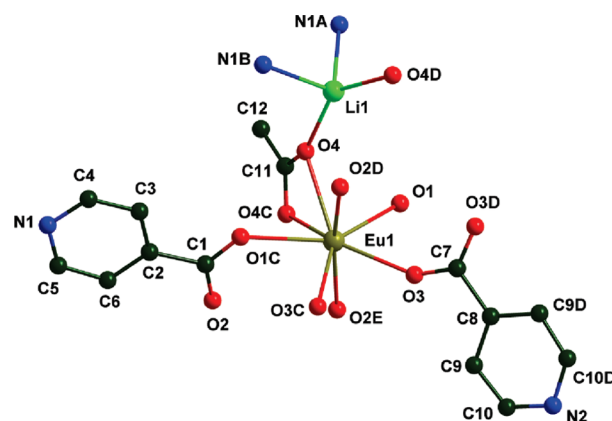

Figure 1. Coordination environments of Eu and Li atoms in **1**. All carbon H atoms are omitted for clarity. Symmetry codes: A ($y, 1 + x, 1/3 − z$); B ($y, 1 − x + y, −1/6 + z$); C ($1 + x − y, 2 − y, −z$); D ($x, 2 + x − y, 1/6 − z$); E ($−1 + y, −x + y, −1/6 + z$).

oxidation of solvent CH_3CN. This interesting organic transformation was observed several times upon repeating a similar reaction, and it could be identified by two main points. First, all the elemental analysis results correspond well with formulas which contain an acetate group; for example, in **1** the calculated CHN percentage for a molecular formula with one acetate group ($C_{20}H_{15}EuLiN_3O_8$) is C, 41.11; H, 2.59; N, 7.19, while including one nitrate group ($C_{18}H_{12}EuLiN_4O_9$) instead of an acetate the ratio changes dramatically to C, 36.38; H, 2.04; N, 9.43. The initial formula corresponds well with the experimental one C, 41.40; H, 2.62; N, 7.03. Second, any effort to crystallographically refine all structures with the employment of the nitrate group, which can be derived from the lanthanide salt, instead of the acetate group, results in an appropriate crystallographic solution; however, the unbounded oxygen atom and the nitrogen atoms of the "nitrate" show nonreasonable thermal parameters in contrast to the crystallographic solution where the acetate groups can be considered as the main coligand. From a synthetic point of view, the source of the alkali metal salts plays an important role in the construction of these compounds. When NaCl and KCl were employed in the reaction system instead of $Na_2C_2O_4$ and KI, the final products did not present any crystallinity. Several efforts have been dedicated to synthesize the Eu−K analogue of **5**; however, all these efforts were unsuccessful.

Crystal Structure of [EuLi(INA)$_3$(OAc)] (1). Single crystal XRD studies revealed that the four compounds **1−4** are isomorphous, so only the structure of **1** is described in detail here. The refined Flack parameter of −0.005(13) shows that the crystal examined has the same handedness throughout its structure, rather than being racemically twinned with different domains containing opposite enantiomers of the network.[8a] Compound **1** displays an unusual 3D chiral heterometallic coordination framework that is built up by right-handed Eu−O−Li chiral helicals and INA linkers, crystallizing in hexagonal space group $P6_122$. There are half of Eu(III) ion, half of Li(I) ion, one and half of INA anions, and half of acetate anion in the asymmetric unit (Figure 1). Each Eu(III) center is coordinated by eight oxygen donors: six oxygen atoms from six INA ligands and the other two oxygen atoms from one OAc ligand. The coordination geometry around the Eu(III) center can be described as a distorted square antiprism geometry with the Eu−O bond lengths varying from 2.3400(17) to 2.4832(18) Å, all

2487

dx.doi.org/10.1021/cg200255r |*Cryst. Growth Des.* 2011, 11, 2485–2492

Scheme 1. Coordination Modes of INA and OAc Ligands in Compounds 1−5
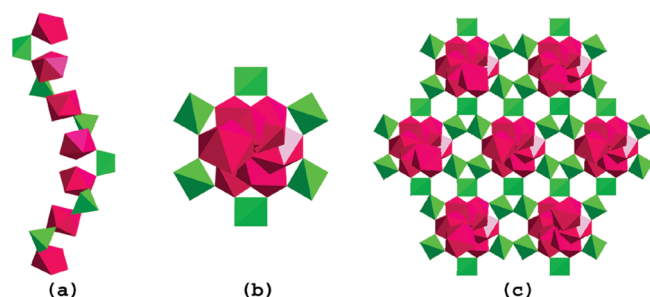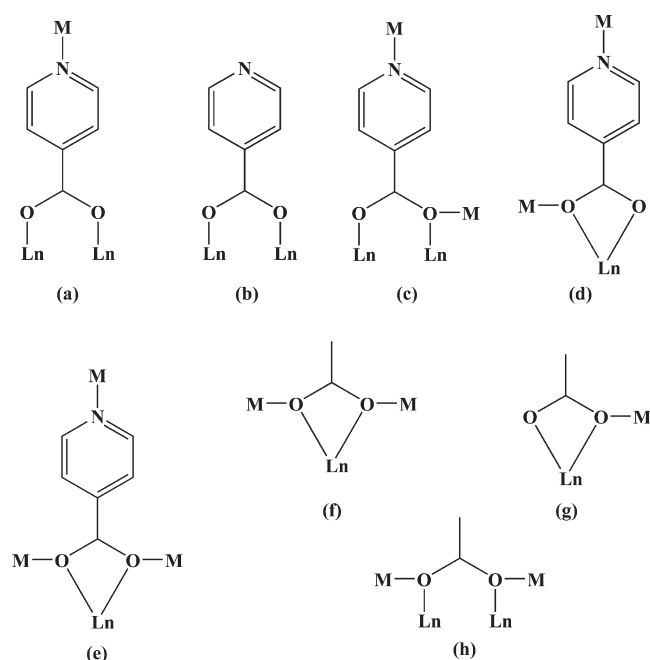
Figure 2. (a) Polyhedral view of the 1D Eu−O−Li heterometallic helical chain in compound **1** along the *b* axis, (b) View of 1D helical chain along the *c* axis, (c) View of the 3D coordination network of compound **1** along the *c* axis (the INA linkers are omitted for clarity).

within the range of those observed for other Eu(III) compounds with oxygen donor ligands.[11] The Li(I) ion is coordinated by two nitrogen atoms from two INA ligands and two oxygen atoms from two OAc ligands to furnish a tetrahedral geometry. The Li−N and Li−O bond lengths are 2.169(5) and 2.084(3) Å (Table 2). The INA ligands in **1** adopt two types of coordination modes: one with the nitrogen atom coordinating to one Li(I) center and the carboxylate connecting to two Eu(III) centers through a bismonodentate fashion (mode a, Scheme 1), the other with the nitrogen atom free and the carboxylate linking to two Eu(III) centers via a bismonodentate mode (mode b, Scheme 1). The OAc ligands chelate to one Eu(III) center and bridge to two Li(I) centers (mode f, Scheme 1). On the basis of the connectivity of organic ligands, a right-hand chiral helical is constructed by the carboxylate oxygen atoms linking the adjacent Li(I) and Eu(III) centers (Figure 2a,b), which contribute to the chirality of the compound. The 6_1 screw axis passes down the center of the helical chain with a pitch of 26.87 Å. Finally, the
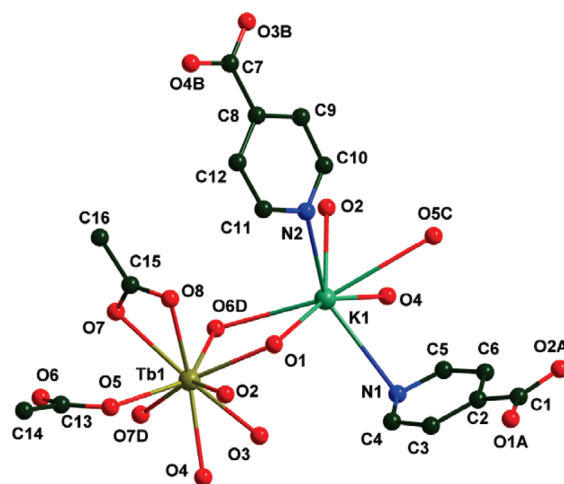
Figure 3. Coordination environments of Tb and K atoms in **5**. All carbon H atoms are omitted for clarity. Symmetry codes: A $(1 − x, 1 − y, −z)$; B $(−1 + x, y, z)$; C $(−1/2 + x, 1/2 − y, −1/2 + z)$; D $(1 − x, −y, −z)$.

Eu−O−Li helical chains are connected together by the INA linkers to form a 3D chiral heterometallic coordination framework (Figure 2c). To the best of our knowledge, this is the first example of a chiral heterometallic coordination polymer assembled by inorganic Eu−O−Li helical chain and organic ligands, though two Ln−O−Ag[6e] and two Ln−O−Cu chains have been reported before.[12] The most striking character of compounds **1**−**4** is the chiral Ln−O−M helical chains, and the adjacent helical chains are linked by the INA ligands to generate a 3D chiral framework. As shown in Figure 2c and Figure S1, one helical chain is interlaced by other six helical chains with the same connectivity, which confirms that acentric helix packing without introduction of an inversion center between them. Helical structural motifs present an axial chirality and packing these 1D helical chains into a 3D chiral framework demands chiral discriminative interactions,[6e,13] the coordination bonds between Ln-O-M helices and INA linkers in compounds **1**−**4** provide the chiral discriminative interactions to realize the chiral assembly.

Crystal Structure of [TbK(INA)₂(OAc)₂] (5). Structure determination shows that compound **5** crystallizes in the monoclinic space group $P2_1/n$ and has a 3D pillared structure that is constructed from 2D Tb−O−K layers with INA as connectivities. There exist one Tb(III) ion, one K(I) ion, two INA ligands, and two acetate anions in the asymmetric unit (Figure 3). Each Tb(III) ion is coordinated by nine oxygen atoms from two INA ligands and four OAc ligands to furnish a distorted tricapped trigonal prism geometry. The Tb−O distances fall in the range of 2.299(2)−2.568(2) Å, compared to those of other terbium-carboxylate compounds.[14] As far as the K(I) ion in the compound is concerned, it presents a monocapped trigonal prism coordinated configuration, being coordinated by two nitrogen atoms and five oxygen atoms from five INA and two OAc ligands. The K−N and K−O bond lengths range from 2.664(3) to 3.162(3) Å (Table 2). In the structure of **5**, the INA ligands adopt two types of coordinated modes: one with the nitrogen atom linking to one K(I) ion and the carboxylate connecting to one Tb(III) ion and one K(I) ion via a chelating and bridging coordinated fashion (mode d, Scheme 1), the other with the nitrogen atom connecting to one K(I) ion and the carboxylate chelating to one Tb(III) ion and bridging to two K(I)
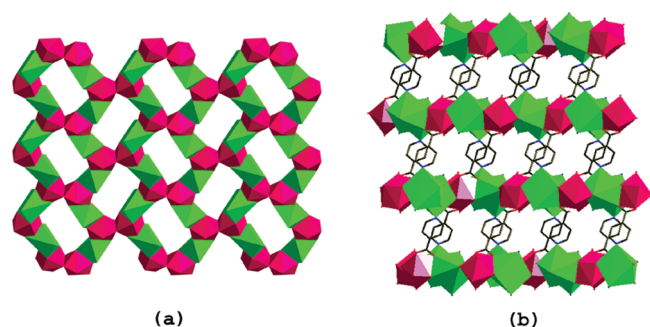
Figure 4. (a) Polyhedral view of the 2D Tb—O—K inorganic hetero-metallic layer in compound **5** along the *a* axis. (b) View of the 3D coordination network of compound **5** along the *b* axis.

ions (mode e, Scheme 1). The OAc ligands also have two types of coordinated fashions: one acts as a chelating and bridging ligand to coordinate to one Tb(III) ion and one K(I) ion (mode g, Scheme 1), and the other also acts as a chelating and bridging ligand to coordinate to two Tb(III) ions and two K(I) ions (mode h, Scheme 1). According to the connectivity of the organic ligands, a 2D inorganic Tb—O—K layer is built up from the alternate Tb(III) and K(I) centers with sharing carboxylate oxygen atoms along the *bc* plane (Figure 4a). The adjacent 2D inorganic Tb—O—K layers are pillared by the INA ligands to form a 3D heterometallic coordination framework (Figure 4b).

A comparison of the final motif of compounds **1**—**5** indicates that the difference in those structures is generated from the size effect of the alkali metal ions. Using the Li(I) and Na(I) ions as precursors, compounds **1**—**4** were constructed, while compound **5** was obtained when the K(I) ion was introduced. The structures of Ln-Li and Ln-Na compounds are very similar except for one type of coordination mode of INA ligands (modes a and c, Scheme 1). In Scheme 1a, the INA ligand only links to two Ln ions via a bis-monodentate mode, while the INA ligand in Scheme 1c not only connects to two Ln ions but also bridges to one Na(I) ion to fill the coordination number of Na(I) ions. Though the difference of the coordination mode of INA ligand did not change the structures of Ln-Li and Ln-Na compounds, the coordination number of alkali metal ions increases with the size of the ions: $LiN_2O_2 < NaN_2O_4 < KN_2O_5$.

Topological Features. As described above, compounds **1**—**4**, despite the fact that they contain different coordination modes of organic ligands, possess similar topology. This feature indicates that the difference in the radii between Li(I) and Na(I) does not affect the shape of the final motif. As described above, the crystal structures of **1**—**4** consist of anionic one-dimensional chains $[Ln(INA)_3(OAc)]^-$ which are extended to three dimensions through Li(I) in **1** and **2** and Na(I) in **3** and **4**; thus, the role of Li(I) and Na(I) is substantial for the growth of the compound to three dimensions, and a logic step for the simplification of the polymeric net is to consider them as a node. Taking into account, for example, in **1**, Li(I) and Eu(III) as a node, the network can thus be presented topologically by a four nodal (3,3,4,7) net.[15a] In this net, each Li(I) atom (blue, Figure 5) represents a 4 connected node, each Eu(III) (light green, Figure 5) represents a 7-connected node, while the two organic ligands (OAc and INA) have been replaced by a 3-connected node (pink, Figure 5). The point symbol of the net is $(3.8^2)_2(3^4.4^2.5^2.6^4.8^5.9^3.10)(5.8^5)(5^2.8)$ and is named as **3,3,4,7T2**. A survey in the TOPOS database[15b] reveals only two compounds (SERYAQ and SERYEU), which possess a similar topology.[6e] Shifting to K(I) as the alkali metal center, the motif
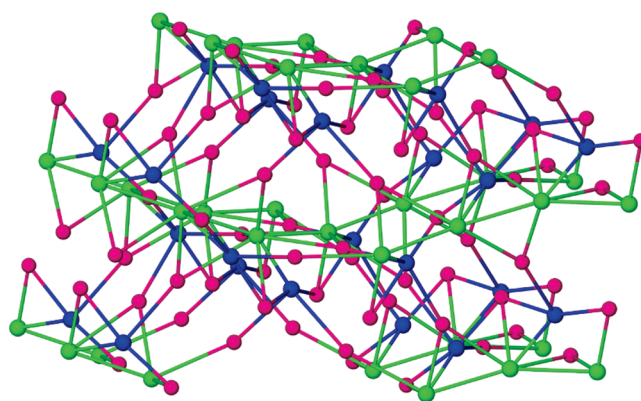

Figure 5. View of the four nodal 3,3,4,7-connected 3D network with **3,3,4,7T2** topology of compound **1** along the *c* axis.
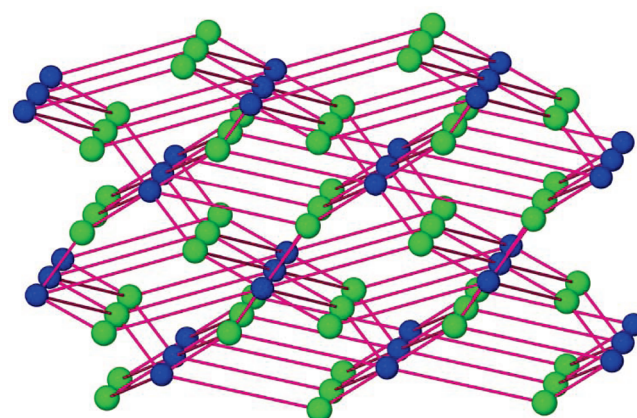
Figure 6. View of the binodal 3D 4,8-connected **alb-4,8-P21/c** network of compound **5**.

of the final product in **5** changes radically. Compound **5** is extended to three dimensions with the employment of all INA ligands. In this case, dianionic dimeric units $\{[Tb(INA)_2(OAc)_2]_2\}^{2-}$ are extended to three dimensions through the K(I) cations. A topological analysis with TOPOS software, considering each K(I) and each dimeric unit as a node, reveals a binodal (4,8) connected net possessing an **alb-4,8-P21/c** topology.[15a] Each K(I) has been replaced as a 4-connected node (light green, Figure 6) and each dimeric unit has been replaced by a 8-connected node (blue, Figure 6). An investigation in the TOPOS database[15b] shows that only five (DEBGIA, LIOXAT, MAQDUD, MAQDUD01, RORQOE) compounds possess a similar topology.[16]

TGA and PXRD. To study the thermal stability of the five compounds, the thermogravimetric analyses of **2**, **4**, and **5** were performed from 35 to 750 °C at a heating rate of 10 °C/min in dry air atmosphere (Figure S2, Supporting Information). The TGA curves of **2** and **4** are similar, suggesting the isomorphous character of **2** and **4**. Compounds **2** and **4** show no weight loss between 35 and 332 °C, indicating the two frameworks can be stable up to 332 °C. Above 332 °C, the framework starts to decompose. Compound **5** undergoes one step of weight loss at about 296 °C attributing to the collapse of the whole framework. Powder X-ray diffraction (PXRD) was used to check the purity of compounds **1**—**5**. As shown in Figure S3, Supporting Information, all the peaks presented in the measured patterns closely match the simulated patterns generated from single-crystal diffraction data, indicating

(a)

(b)

(c)
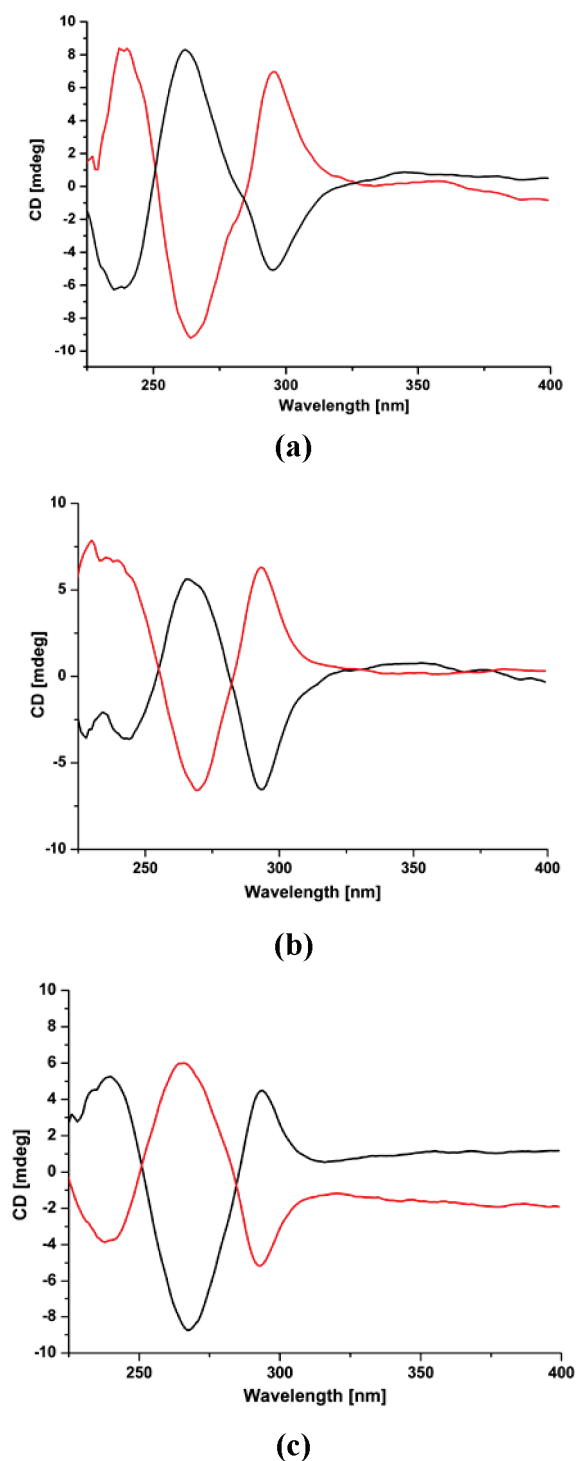
Figure 7. Solid-state CD spectra of compounds (a) **1**, (b) **3**, and (c) **4** at room temperature.

single phases of **1−5** are formed. The PXRD patterns of compounds **1−4** are very similar as well, further confirming the isostructural nature of the four compounds.

CD Spectra. The solid-state CD spectra of compounds **1**, **3**, and **4** were recorded on single crystals with KCl pellets between 200 and 400 nm at room temperature (Figure 7). The CD spectra of **1**, **3**, and **4** present an obvious Cotton effect. The crystals of **1** exhibit opposite Cotton effects at the same wavelengths (three

(a)

(b)
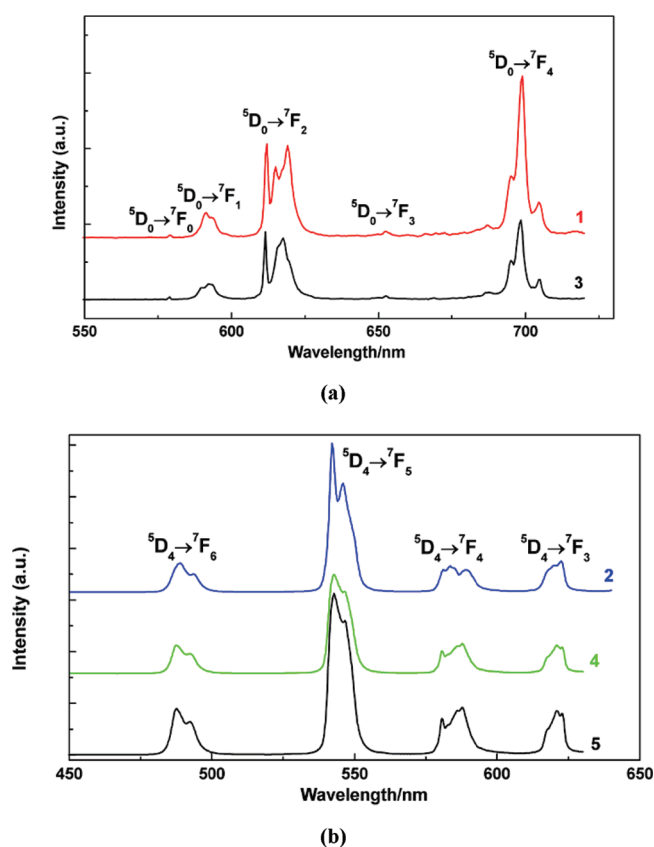
Figure 8. (a) Emission spectra of compounds **1** and **3**. (b) Emission spectra of compounds **2**, **4**, and **5**.

peaks at 237, 264, and 296 nm), indicating the coexistence of left-hand and right-handed enantiomers in one pot, which confirms spontaneous resolution during the course of the crystallization. The curves of **3** and **4** are very similar to **1**. To further investigate whether the enantiomeric excess exists in these chiral crystals, the bulk sample of **1** was measured by CD spectrum; however, each bulk sample of **1** showed a silent CD spectrum (Figure S4, Supporting Information). All the results confirmed that the resulting crystals of **1−4** were racemic mixtures.

Photoluminescent Properties. The luminescent spectra of compounds **1−5** were investigated in the solid state at room temperature (Figure 8). Under excitation at 394 nm, compounds **1** and **3** yield intense red luminescence. Compound **1** exhibits characteristic peaks at 579, 592, 615, 651, and 699 nm, while compound **3** presents characteristic peaks at 579, 592, 617, 653, and 698 nm, all of which are assigned to the transition of $^5D_0 \rightarrow {}^7F_J$ ($J = 0 \rightarrow 4$) of the Eu(III) ion. The symmetric forbidden emission $^5D_0 \rightarrow {}^7F_0$ at 579 nm appears in **1** and **3**, indicating that the Eu(III) ion occupies sites without inversion symmetry. The $^5D_0 \rightarrow {}^7F_2$ transition is stronger than the $^5D_0 \rightarrow {}^7F_1$ transition, which suggests that the Eu(III) ions have a low symmetric coordination environment.[17] This is consistent with the result of the single-crystal X-ray analysis. Compounds **2**, **4**, and **5** display green luminescence with typical emission of Tb(III) ion at 489, 542, 583, 622 nm; 487, 543, 587, 621 nm and 488, 543, 587, 622 nm, respectively, attributing to electronic transitions from the excited state $^5D_4$ to the multiplets ^7F_J ($J = 6 \rightarrow 3$). The dominant band is the hypersensitive transition $^5D_4 \rightarrow {}^7F_5$ of Tb(III) ion in compounds **2**, **4**, and **5**, which consists of an intense peak with a shoulder.[18]

■ CONCLUSION

A series of chiral and achiral lanthanide-alkali heterometallic coordination polymers have been solvothermally synthesized and structurally characterized. The structural differences among compounds **1−5** highlight the effect of alkali metal ions on their framework construction. Compounds **1−4** are isostructural 3D coordination polymers and built up by right-/left-handed Ln-O-M chiral helicals and INA linkers possessing an **3,3,4,7T2** topology, while compound **5** is a 3D pillared coordination polymer constructed from 2D Tb−O−K layers with INA as connectivities possessing a **alb-4,8-P21/c** topology. To the best of our knowledge, the systematic study of chiral or achiral lanthanide-alkali heterometallic coordination polymers influenced by alkali metal ions has not been reported before. The successful preparation of the five compounds provides a valuable approach for the construction of other novel chiral or achiral lanthanide-alkali metal coordination polymers with interesting structures, topologies, and optical properties.

■ ASSOCIATED CONTENT

ⓈSupporting Information. X-ray crystallographic files in CIF format for structures **1−5**, TGA curves, PXRD patterns, and additional figures. This material is available free of charge via the Internet at http://pubs.acs.org.

■ AUTHOR INFORMATION

Corresponding Authors
*E-mail: dh@scnu.edu.cn (H.D.), George.Kostakis@kit.edu (G.E.K.).

■ ACKNOWLEDGMENT

■ REFERENCES

(1) (a) Ma, L. Q.; Abney, C.; Lin, W. B. *Chem. Soc. Rev.* **2009**, *38*, 1248. (b) Lee, S. J.; Lin, W. *Acc. Chem. Res.* **2008**, *41*, 521. (c) Ye, Q.; Wang, X. S.; Zhao, Hong.; Xiong, R. G. *Chem. Soc. Rev.* **2005**, *34*, 208. (d) Kesanli, B.; Lin, W. *Coord. Chem. Rev.* **2003**, *246*, 305. (e) Lin, W. *MRS Bull.* **2007**, *32*, 544. (f) Seo, J. S.; Whang, D.; Lee, H.; Jun, S.; Oh, J.; Jeon, Y.; Kim, K. *Nature* **2000**, *404*, 982. (g) Xiong, R. G.; You, X. Z.; Abrahams, B. F.; Xue, Z. L.; Che, C. M. *Angew. Chem., Int. Ed.* **2001**, *40*, 4422.

(2) (a) Amabilino, D. B.; Veciana, J. *Top. Curr. Chem.* **2006**, *265*, 253. (b) Guo, Z.; Cao, R.; Wang, X.; Li, H.; Yuan, W.; Wang, G.; Wu, H.; Li, J. *J. Am. Chem. Soc.* **2009**, *131*, 6894. (c) Zhao, H.; Qu, Z. R.; Ye, H. Y.; Xiong, R. G. *Chem. Soc. Rev.* **2008**, *37*, 84. (d) Zhang, W.; Xiong, R. G.; Huang, S. D. *J. Am. Chem. Soc.* **2008**, *130*, 10468. (e) Xie, Y. M.; Liu, J. H.; Wu, X. Y.; Zhao, Z. G.; Zhang, Q. S.; Wang, F.; Chen, S. C.; Lu, C. Z. *Cryst. Growth Des.* **2008**, *8*, 3914.

(3) (a) Train, C.; Gheorghe, R.; Krstic, V.; Chamorerau, L. M.; Ovanesyan, N. S.; Rikken, G. J. A.; Gruselle, M.; Verdaguer, M. *Nat. Mater.* **2008**, *7*, 729. (b) Gao, E. Q.; Yue, Y. F.; Bai, S. Q.; He, Z.; Yan, C. H. *J. Am. Chem. Soc.* **2004**, *126*, 1419. (c) Wen, H. R.; Tang, Y. Z.; Liu, C. M.; Chen, J. L.; Yu, C. L. *Inorg. Chem.* **2009**, *48*, 10177. (d) Inoue, K.; Kikuchi, K.; Ohba, M; Ōkawa, H. *Angew. Chem., Int. Ed.* **2003**, *42*, 4810.

(4) (a) Chin, J.; Lee, S. S.; Lee, K. J.; Park, S.; Kim, D. H. *Nature* **1999**, *401*, 254. (b) Rivera, J. M.; Martín, T.; Rebek, J., Jr. *Science* **1998**, *279*, 1021. (c) Wang, X. W.; Han, L.; Cai, T. J.; Zheng, Y. Q.; Chen, J. Z.; Deng, Q. *Cryst. Growth Des.* **2007**, *7*, 1027.

(5) (a) Zhang, J.; Chen, S.; Bu, X. *Angew. Chem., Int. Ed.* **2008**, *47*, 5434. (b) Zhang, J.; Chen, S.; Zingiryan, A.; Bu, X. *J. Am. Chem. Soc.* **2008**, *130*, 17246. (c) Liu, Y.; Xuan, W.; Zhang, H.; Cui, Y. *Inorg. Chem.* **2009**, *48*, 10018. (d) Ryoo, J. J.; Shin, J. W.; Dho, H. S.; Min, K. S. *Inorg. Chem.* **2010**, *49*, 7232. (e) Amghouz, Z.; Roces, L.; García-Granda, S.; García, J. R.; Souhail, B.; Mafra, L.; Shi, F.; Rocha, J. *Inorg. Chem.* **2010**, *49*, 7917. (f) Wang, Y.; Fu, H.; Shen, F.; Sheng, X.; Peng, A.; Gu, Z.; Ma, H.; Ma, J.; Yao, J. *Inorg. Chem.* **2007**, *46*, 3548. (g) Li, X.; Liu, T.; Hu, B.; Li, G.; Zhang, H.; Cao, R. *Cryst. Growth Des.* **2010**, *10*, 3051. (h) Ou, G. C.; Jiang, L.; Feng, X. L.; Lu, T. B. *Inorg. Chem.* **2008**, *47*, 2710.

(6) (a) Lennartson, A.; Håkansson, M. *Angew. Chem., Int. Ed.* **2009**, *48*, 5869. (b) Hou, S. Z.; Cao, D. K.; Li, Y. Z.; Zheng, L. M. *Inorg. Chem.* **2008**, *47*, 10211. (c) Liang, X. Q.; Jia, J. T.; Wu, T.; Li, D. P.; Liu, L.; Tsolmona; Zhu, G. S. *CrystEngComm* **2010**, *12*, 3499. (d) Su, Z.; Chen, M. S.; Fan, J.; Chen, M.; Chen, S. S.; Luo, L.; Sun, W. Y. *CrystEngComm* **2010**, *12*, 2040. (e) Gu, X.; Xue, D. *Inorg. Chem.* **2006**, *45*, 9257. (f) Han, Z. B.; Ji, J. W.; An, H. Y.; Zhang, W.; Han, G. X.; Zhang, G. X.; Yang, L. G. *Dalton Trans.* **2009**, 9807. (g) Lennartson, A.; Vestergren, M.; Håkansson, M. *Chem.—Eur. J.* **2005**, *11*, 1757. (h) Martin, D. P.; Staples, R. J.; LaDuca, R. L. *Inorg. Chem.* **2008**, *47*, 9754.

(7) (a) Paler, A. R. *Science* **2004**, *306*, 828. (b) Brown, J. M.; Davies, S. G. *Nature* **1989**, *342*, 631. (c) Feringa, B. L.; Delden, R. A. *Angew. Chem., Int. Ed.* **1999**, *38*, 3418. (d) Kondepudi, D. K.; Asakura, K. *Acc. Chem. Res.* **2001**, *34*, 946. (e) Wu, S. T.; Wu, Y. R.; Kang, Q. Q.; Zhang, H.; Long, L. S.; Zheng, Z.; Huang, R. B.; Zheng, L. S. *Angew. Chem., Int. Ed.* **2007**, *46*, 8475.

(8) (a) Majeed, Z.; Mondal, K. C.; Kostakis, G. E.; Lan, Y.; Anson, C. E.; Powell, A. K. *Chem. Commun.* **2010**, *46*, 2551. (b) Kostakis, G. E.; Powell, A. K. *Dalton Trans.* **2010**, *39*, 2249. (c) Sendor, D.; Hilder, M.; Juestel, T.; Junk, P. C.; Kynast, U. H. *New J. Chem.* **2003**, *27*, 1070. (d) Wooten, A. J.; Carroll, P. J.; Walsh, P. J. *Org. Lett.* **2007**, *9*, 3359.

(9) (a) Peng, G.; Qiu, Y. Q.; Liu, Z. H.; Liu, B.; Deng, H. *Cryst. Growth Des.* **2010**, *10*, 114. (b) Peng, G.; Ma, L.; Liu, B.; Cai, J. B.; Deng, H. *Inorg. Chem. Commun.* **2010**, *13*, 599. (c) Qiu, Y.; Liu, Z.; Mou, J.; Deng, H.; Zeller, M. *CrystEngComm* **2010**, *12*, 277. (d) Liu, B.; Qiu, Y. Q.; Peng, G.; Deng, H. *CrystEngComm* **2010**, *12*, 270.

(10) (a) *Bruker APEXII software*, Version 6.12; Bruker AXS Inc.: Madison, Wisconsin, USA, 2004. (b) Sheldrick, G. M. *SHELXL-97, Program for X-ray Crystal Structure Refinement*; University of Göttingen: Göttingen, Germany, 1997.

(11) (a) Xiang, S.; Hu, S.; Sheng, T.; Chen, J.; Wu, X. *Chem.—Eur. J.* **2009**, *15*, 12496. (b) Zhao, X. Q.; Zuo, Y.; Gao, D. L.; Zhao, B.; Shi, W.; Cheng, P. *Cryst. Growth Des.* **2009**, *9*, 3948. (c) Cao, D. K.; Hou, S. Z.; Li, Y. Z.; Zheng, L. M. *Cryst. Growth Des.* **2009**, *9*, 4445. (d) Gu, X. J.; Xue, D. F. *Cryst. Growth Des.* **2007**, *7*, 1726. (e) Sun, Y. Q.; Zhang, J.; Yang, G. Y. *Chem. Commun.* **2006**, 4700.

(12) Cutland-Van Noord, A. D.; Kampf, J. W.; Pecoraro, V. L. *Angew. Chem., Int. Ed.* **2002**, *41*, 4668.

(13) (a) Piguet, C.; Bernardinelli, G.; Hopfgartner, G. *Chem. Rev.* **1997**, *97*, 2005. (b) Custelcean, R.; Ward, D. W. *Cryst. Growth Des.* **2005**, *5*, 2279.

(14) (a) Huang, Y. G.; Wang, X. T.; Jiang, F. L.; Gao, S.; Wu, M. Y.; Gao, Q.; Wei, W.; Hong, M. C. *Chem.—Eur. J.* **2008**, *14*, 10340. (b) Zhao, X. Q.; Zhao, B.; Shi, W.; Cheng, P. *Inorg. Chem.* **2009**, *48*, 11048. (c) Zhou, X. H.; Peng, Y. H.; Du, X. D.; Wang, C. F.; Zuo, J. L.; You, X. Z. *Cryst. Growth Des.* **2009**, *9*, 1028. (d) Luo, F.; Long, G. J.; Che, Y. X.; Zheng, J. M. *Cryst. Growth Des.* **2008**, *8*, 3511.

(15) (a) Blatov, V. A. *IUCr CompComm Newsletter*, **2006**, *7*, 4; (b) Alexandrov, E. V.; Blatov, V. A.; Kochetkov, A. V.; Proserpio, D. M. *CrystEngComm*, **2011**, DOI: 10.1039/c0ce00636j.

(16) (a) Kondo, M.; Shimamura, M.; Noro, S.; Yoshitomi, T.; Minakoshi, S.; Kitagawa, S. *Chem. Lett.* **1999**, 285. (b) Beagley, B.; Small, R. W. H. *Acta Crystallogr.* **1964**, *17*, 783. (c) Kaduk, J. A. *Acta Crystallogr., Sect. B* **2000**, *56*, 474. (d) Frenzer, W.; Wartchow, R.; Bode, H. *Z. Kristallogr.* **1997**, *212*, 237.

(17) (a) Bünzli, J. C. G.; Choppin, G. R. Lanthanide Probes in Life, *Chemical and Earth Sciences. Theory and Practice*; Elsevier Scientific Publishers: Amsterdam, The Netherlands, 1989; Chapter 7. (b) Bünzli, J. C. G.; Piguet, C. *Chem. Soc. Rev.* **2005**, *34*, 1048. (c) Gunning, N. S.; Cahill, C. L. *Dalton Trans.* **2005**, 2788.

(18) (a) Richardson, F. S. *Chem. Rev.* **1982**, *82*, 541. (b) Bo, Q. B.; Sun, G. X.; Geng, D. L. *Inorg. Chem.* **2010**, *49*, 561.

2492

dx.doi.org/10.1021/cg200255r |*Cryst. Growth Des.* 2011, 11, 2485–2492